

# CHARACTERISTICS ON HDS AND HDN KINETICS OF NARROW FRACTIONS FROM RESIDUA

Chaohu Yang, Feng Du, Chunming Xu  
State Key Laboratory of Heavy Oil Processing, University of Petroleum  
Dongying city, Shandong province, 257062 China

## ABSTRACT

An atmospheric residuum from Dagang crude of China (DGAR) and two vacuum residua from Arabian Light crude and Arabian Medium crude (SQVR and SZVR) were fractionated into 7-8 cuts by supercritical fluid extraction fractionation (SFEF) technique developed by State Key Laboratory of Heavy Oil Processing. These SFEF fractions were catalytically hydroprocessed in a 100 mL autoclave with crushed commercial Ni-Mo catalyst. The HDS and HDN diffusion-reaction model of residue in autoclave reactor was established. The diffusion and HDS and HDN characteristics of these fractions were discussed.

**KEYWORDS:** heavy oil, diffusion, HDS and HDN

## INTRODUCTION

Because of the increase of heavy oils and bitumen as refinery feedstock and the growing demand of amount and quality for light distillate oils, catalytic hydroprocessing of heavy oil plays a growingly important role in modern petroleum deeply processing. Considerable effort has been focused worldwide on characterizing oils from the points of view of feedstock properties and the resultant kinetic properties. Much of this effort, however, has been directed at characterizing the reaction kinetics of whole oils, and the investigations about the hydroconversion features of narrow fractions of heavy oils are scarce. Hoog(1950)<sup>[1]</sup>, Yitzhaki and Aharoni(1988)<sup>[2]</sup>, Papayannakos(1988)<sup>[3]</sup>, and Trytten & Gray(1990)<sup>[4]</sup> studied the hydroconversion of narrow fractions from distillates. The removal of sulfur and nitrogen as well as conversion of aromatic carbon decreases with the increase of average molecular weight (AMW) of feed. Although the hydroconversion is affected by its intrinsic reactivity and diffusion property, the intrinsic reactivity is the controlling factor of reaction rate, especially for the heavier fractions. In a small reactor designed oneself, Dai<sup>[5]</sup> investigated the resin catalytic cracking of each SFEF fraction from Shengli Vacuum residuum. When the total yield of extract oil in SFEF is not greater than 78%, the resin in each fraction can be cracked easily with a liquid yield of 65-75%. The reactivity of resin is greatly affected by its AMW, the greater the AMW of resin is, the poorer the cracking reactivity.

As a whole, the reaction feature of feed varies with the AMW, or molecular size. Now there is not investigation about the hydroconversion characteristics of narrow fractions of residuum reported for lack of proper separation method. The SFEF technique developed by State Key Laboratory of Heavy Oil Processing affords the possibility to do such a work. In this paper, three residua were fractionated into narrow fractions by the SFEF method and the hydroconversion characteristics of every fraction were studied at the same conditions.

## EXPERIMENTAL

**Feedstocks** Two vacuum residua of Arabian Light crude and Arabian medium crude were provided by Fushun Research Institute of Petroleum Processing, and Dagang atmospheric residuum came from Dagang refinery. Such three residua were separated respectively into 8 fractions by the SFEF method. The main properties of each fraction were measured, density at 20°C is of 0.8721 to 1.1405g/cm<sup>3</sup>, AMW of 353-3394, sulfur of 0.101-6.40 m%, nitrogen of 436-9700 µg/g, H/C atomic ratio of 1.40-1.81.

**Catalyst** A key catalyst used in Chevron VRDS process (CAT1) and another catalyst (CAT2) produced in China were chosen in this research. The average pore diameter of both catalysts is 33Å and 38Å, pore volume is 0.45 and 0.39mL/g, and specific surface area is 275 and 203m<sup>2</sup>/g. The main metal active components are molybdenum and nickel. Catalyst was crushed and sieved into 60/80 mesh particles (average diameter of 0.35mm), and the catalyst particles were presulfurized before use in reaction.

**Hydroconversion and Separation** The crushed catalyst was presulfurized firstly, washed with solvent and dried in a vacuum drying oven. The presulfurized catalyst and sample were charged into the autoclave with the ratio of 1 to 10. Reaction conditions were set as follows: 400°C 8.5Mpa of initial hydrogen pressure, 4 hours and 850rpm of agitation rate. After loading the catalyst and sample, the system was purged with hydrogen three times, then the temperature was increased gradually and the agitator was switched on when the temperature reached from 100° - 150°C. After reaction, the autoclave was taken out from the heating furnace and put it into cooling water. When the temperature reaches to about 200°C, the reactor was placed into an isothermal water bath of 60°C in order to assure the consistency of sampling conditions and avoid or reduce the evaporation of light components in liquid product. While the autoclave comes to about 60°C, reactor was connected to a gas ration and sampling system for collecting gas product. The in-situ temperature, atmospheric pressure and the collected gas volume were recorded. Then the gas product was transferred into a gas sample bag for composition analysis. After sampling gas, the reactor was cooled down to ambient temperature, opening the reactor and taking immediately a little liquid product into a centrifugal test tube. The catalyst contained in the liquid product was deposited on the bottom of the test tube by centrifugation separation in a centrifugal machine at 5000rpm for 5 minutes. The upper oil in test tube was transferred to a sealed vial for simulated distillation analysis.

The remaining liquid product and catalyst in reactor was diluted with solvent and transferred into a Soxhlet apparatus, then extracted with dichloro-ethane for one hour, finally the extracted liquid should be not color. The wet catalyst in the extractor was taken out and placed into a vacuum drying oven to dry for coke content and other properties analysis. The extractive was distilled at atmospheric pressure to recover the solvent, then the liquid product was transferred into a small distillation flask of 150mL and subjected to vacuum distillation to obtain the high boiling residue of >350°C for analyzing the sulfur and nitrogen contents, molecular weight, and hydrocarbon group composition.

In the present study, the loss in experiment could be ignorable, and sum of yields of gas, coke and liquid product accounted as 100%. Once the gas and coke yields are determined, the yield of any distillate can be calculated according to the simulated distillation data of liquid product.

## DIFFUSION-REACTION MODEL

**Reaction Kinetic Model** The non-homogenous catalytic reaction with order of n can be described generally as follows:

$$r = -\frac{dN}{dt} \cdot \frac{1}{w_c \cdot s_g} = k_s \cdot c_m^n \quad (1)$$

Where, r--amount consumed on unit surface area of catalyst in unit time, mol/(m<sup>2</sup>·s);

N--amount of reactant, mol

t--reaction time, s;

w<sub>c</sub>--catalyst weight, g;

s<sub>g</sub>--specific surface area of catalyst, m<sup>2</sup>/g

c<sub>m</sub>--concentration of reactant, mol/m<sup>3</sup>;

k<sub>s</sub>--apparent rate constant for first-order reaction based on the surface area of catalyst, m<sup>3n</sup>/(mol<sup>(n-1)</sup>·m<sup>2</sup>·s)

If the volume of reaction mixture is thought changeless in reaction process, the right end of equation above can be written as,

$$\frac{dN}{dt} \cdot \frac{1}{w_c \cdot s_g} = \frac{d(c_m \cdot v_r)}{dt} \cdot \frac{1}{w_c \cdot s_g} = \frac{v_r \cdot dc_m}{w_c \cdot s_g \cdot dt}$$

That is,

$$-\frac{dc_m}{dt} = \frac{w_c \cdot s_g}{v_r} \cdot k_s \cdot c_m^n \quad (2)$$

When v<sub>r</sub> is the volume of reaction mixture(m<sup>3</sup>). The molar concentration of reactant is converted

into mass fraction,  $c = \frac{c_m \cdot M}{\rho_r}$

Where, c--the mass fraction of reactant ;

M--molecular weight of reactant/g mol<sup>-1</sup>;

ρ<sub>r</sub>--density of reaction mixture at reaction temperature/gm<sup>3</sup>.

Substitution of the above relation in equation (2) gives,

$$-\frac{dc}{dt} = \frac{w_c \cdot s_g}{v_r} \cdot \left(\frac{\rho_r}{M}\right)^{n-1} \cdot k_i \cdot c^n \quad (3)$$

In the special case of  $n=1$ , equation (3) reduces to

$$-\frac{dc}{dt} = \frac{w_c \cdot s_g}{v_r} \cdot k_s \cdot c \quad (4)$$

Integrating equation (4), we get,

$$\ln \frac{c_0}{c} = \frac{w_c \cdot s_g}{v_r} \cdot k_s \cdot t \quad (5a)$$

or

$$-\ln(1-x) = \frac{w_c \cdot s_g}{v_r} \cdot k_s \cdot t \quad (5b)$$

Where  $x$  is the conversion of reactant  $x = (c_0 - c) / c_0$ . Solving the  $k_s$  From equation (5b) gives

$$k_s = -\frac{v_r \cdot \ln(1-x)}{w_c \cdot s_g \cdot t} \quad (6)$$

Many investigators<sup>[6]</sup> have correlated their experimental data with first-order kinetics for the HDS and HDN reactions of residua. In general, the conversions of HDS and HDN are not greater than 90% in this study, and the feed with narrow range has similar reactivity for all compounds contained in it. For simplicity, HDS and HDN are treated as first-order irreversibly reactions, so the apparent rate constants can be calculated by equation (6).

**Diffusion Effect** The external diffusion effect on reaction rate is ignorable in the stirred autoclave with high agitation speed<sup>[7]</sup>. The effect of reactant migration through catalyst micropores on reaction rate can be described by the effectiveness factor,

$$\eta = \frac{\text{actual reaction rate within pore}}{\text{rate of not slowed by pore diffusion}} \quad (7)$$

For first-order reaction, the relationships between effectiveness factor and Thiele modulus have been proposed for different catalyst shape.

$$\text{Single cylindrical pore}^{[8]} \quad \eta = \frac{\tanh(\phi)}{\phi} \quad (8)$$

$$\text{Long cylinder particle}^{[9]} \quad \eta = \frac{1}{\phi} \frac{I_1(2\phi)}{I_2(2\phi)} \quad (9)$$

$$\text{Sphere particle}^{[10]} \quad \eta = \frac{1}{\phi} \left[ \frac{1}{\tanh(3\phi)} - \frac{1}{3\phi} \right] \quad (10)$$

$$\phi = \frac{V_p}{A_p} \cdot \left( \frac{\rho_p \cdot s_g \cdot k_i}{D_e} \right)^{1/2} \quad (11)$$

Where,  $\phi$ —Thiele modulus, dimensionless

$V_p$ —volume of catalyst particle,  $m^3$

$A_p$ —external surface area of catalyst particle,  $m^2$

$\rho_p$ —particle density of catalyst,  $g/m^3$

$k_i$ —intrinsic rate constant based on the surface area of catalyst,  $m/s$

$D_e$ —effective diffusion coefficient of reactant,  $m^2/s$ .

Although the forms of three equations above for different shape of catalyst particle are different, the predicted values of  $\eta$  at the same  $\phi$  are similar, especially for the case of  $\phi < 4$ . In the present study, equation(10) for sphere particle was selected to describe the relationship of effectiveness factor of HDS and HDN reactions and Thiele modulus.

Assuming no temperature gradient exists between the external surface and the center of catalyst particle, for first-order irreversible reaction we have,

$$\eta = \frac{k_s}{k_i} \quad (12)$$

$$\text{for sphere catalyst particle} \quad \frac{V_p}{A_p} = \frac{d_p}{6} \quad (13)$$

where  $d_p$  is the equivalent sphere diameter(m). Substitution of equation (11), (12) and (13) in

equation (10) gives,

$$\frac{k_s}{k_i} = \frac{3}{Ak_i^{0.5}} \left[ \frac{1}{\tanh(Ak_i^{0.5})} - \frac{1}{Ak_i^{0.5}} \right] \quad (14)$$

where,

$$A = \frac{d_p}{2} \left( \frac{\rho_p \cdot s_g}{D_e} \right)^{1/2} \quad (15)$$

If the parameter  $d_p$ ,  $\rho_p$ ,  $s_g$ ,  $v_r$ ,  $w_c$ ,  $t$  and  $x$  in equation (6), (14), (15) are obtained, the apparent rate constant  $k_3$  can be calculated by equation (6), parameter A can be determined once the effective diffusivity is given. Instituting  $k_s$  and A into equation (14), the intrinsic rate constant,  $k_i$ , can be calculated by Newton iteration, and the effectiveness factor,  $\eta$ , will be determined by equation (12).

**Estimation of Effective Diffusivity** For heavy oil hydroconversion, three phases of gas, liquid and solid exist simultaneously, the reactant must firstly migrate through the micropores filled with liquid to the internal surface of catalyst, and then the catalytic reactions take place there. The transport in liquid-filled pores is usually described by a Fickian diffusion relation with a effective diffusion coefficient<sup>[11]</sup> ( $D_e = \frac{\epsilon}{\tau} D_b$ ). When the size of diffusion molecules and the pores are of the same order of magnitude, the interaction between the walls and coefficient tends to decrease the effective diffusivity. It belongs to the configuration diffusion and the effective diffusivity can be computed by the equation,

$$D_e = \frac{\epsilon}{\tau} D_b \cdot F(\lambda) \quad (16)$$

Where  $D_e$ —effective diffusion coefficient,  $m^2/s$ ;  
 $D_b$ —bulk diffusion coefficient,  $m^2/s$ ;  
 $\epsilon$ —catalyst porosity,  $\epsilon = V_g \cdot \rho_p$ ;  
 $V_g$ —pore volume of catalyst,  $m^3/g$   
 $\tau$ —catalyst tortuosity which have a value of 1-6, For catalysts in this study,  $\tau$  was set to be equal to 4 according to the reference<sup>[10]</sup>.

$F(\lambda)$  is named as restricted diffusion Factor,  $F(\lambda) = k_p \cdot k_r$ <sup>[12]</sup>.  $k_p$  is the ratio between the concentration of diffusion molecules inside and outside the pore and depends on  $\lambda$ , the ratio of pore to molecule diameter. For small solvent molecules,  $k_p$  satisfies the relation:  $k_p = (1 - \lambda)^2$ . When either the solute or the solvent absorb on the surface of pore, there is a resistance caused by drag exerted on the moving molecules by the walls. This influence is expressed through the drag coefficient,  $k_r$ .

Some relation of  $F(\lambda)$  and  $\lambda$  were summarized in chapter I of reference [13], which are illustrated schematically in figure 1. Figure 1 shows that the theoretical model proposed by Renkin is very close to the experimental model developed by Lee through the kinetic experiment. Here the Renkin's relation was chosen to computer the restricted diffusion factor.

$$F(\lambda) = (1 - \lambda)^2 \cdot (1 - 2.104\lambda + 2.09\lambda^3 - 0.95\lambda^5), \quad \lambda < 0.5 \quad (17)$$

Bulk diffusion coefficient is calculated by Stokes-Einstein equation<sup>[14]</sup>,

$$D_b = \frac{kT}{3\pi \cdot \mu \cdot d_r} \quad (18)$$

Where,  $k$ —Boltzmann constant,  $1.38 \times 10^{-23} J / K$ ;  
 $T$ —absolute temperature,  $K$ ;  
 $d_r$ —diameter of spherical solute,  $m$ ;  
 $\mu$ —viscosity of solvent,  $Pa \cdot s$ .

The empirical relation between the equivalent spherical diameter and the molecular weight was selected to estimate the size of reactant<sup>[13]</sup>,

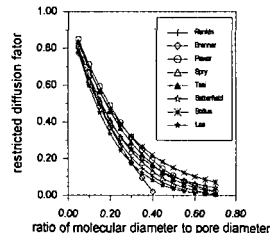


Fig.1  $F(\lambda)$  versus  $\lambda$

$$d_r = 0.403 \cdot M^{0.537}$$

(19)

In industrial process, all molecules with different size exist in one system with the same viscosity of solvent. The viscosity of reactant mixture was estimated to be  $1.24 \times 10^{-4} \text{ Pa} \cdot \text{s}$  under  $390^\circ\text{C}$ , 7.6MPa in the study of residuum hydroprocessing. In the present study, every SEFE fraction was subject to hydroconversion, then the viscosity of reaction system may be different for different fraction. The viscosity of feed and product at reaction conditions was calculated using ASPEN software, and the viscosity in equation (18) was taken as an average of calculated viscosity of feed and product. The deviation of the viscosity for heaviest fractions may be larger for lack of distillation data of feed.

Now, the effective diffusivity can be determined through equations (19), (18), (17) and (16).

## RESULTS AND DISCUSSION

The reaction product was classified into two lumps, the heavy lump of  $>350^\circ\text{C}$  and the light lump of  $<350^\circ\text{C}$ . The sulfur and nitrogen in light lump migrated from heavy lump were thought removal by hydrogenation. Therefore, the conversion of HDS and HDN can be calculated according to the distillation data and the element analysis results.

The equivalent spherical diameter, bulk diffusion coefficient, effective diffusivity, effectiveness factor, apparent and intrinsic rate constant of HDS and HDN were obtained for every SEFE fraction in terms of the diffusion-reaction model mentioned above. The result was summarized in table 1.

Table 1A HDS diffusivities and kinetic parameters of SFEF fractions

feed	$d_r/\text{\AA}$	$F(\lambda)$	$D_b/10^{-10}\text{m}^2\text{s}^{-1}$	$D_e/10^{-10}\text{m}^2\text{s}^{-1}$	$k/10^{-4}\text{ms}^{-1}$	$k_p/10^{-4}\text{ms}^{-1}$	$\eta$
DGAR-1	9.34	0.522	112.2	10.01	9.250	9.323	0.992
DGAR-2	9.71	0.507	93.53	8.109	8.894	8.978	0.990
DGAR-3	10.1	0.492	85.27	7.175	8.405	8.490	0.990
DGAR-4	10.3	0.483	76.00	6.274	8.087	8.177	0.989
DGAR-5	10.6	0.474	72.30	5.858	8.242	8.341	0.988
DGAR-6	10.8	0.462	63.83	5.046	7.626	7.725	0.987
DGAR-7	11.3	0.445	51.71	3.936	6.949	7.055	0.985
DGAR-8	12.2	0.413	27.55	1.946	6.664	6.862	0.971
DGAR residue	20.2	0.198	2.116	0.072	1.641	1.997	0.821
DGAR	11.0	0.456	62.23	4.856	4.261	4.293	0.992
SZVR-1	11.2	0.448	38.48	2.949	7.267	7.422	0.979
SZVR-2	12.5	0.402	7.207	0.495	5.496	6.045	0.909
SZVR-3	13.1	0.385	6.894	0.454	3.463	3.697	0.936
SZVR-4	13.6	0.367	5.141	0.322	3.969	4.411	0.899
SZVR-5	14.5	0.339	3.415	0.197	2.007	2.189	0.916
SZVR-6	14.8	0.332	2.582	0.146	2.178	2.475	0.880
SZVR-7	17.1	0.269	1.761	0.081	1.475	1.725	0.855
SZVR residue	31.7	0.053	0.772	0.0069	0.785	1.839	0.426
SQVR-2	12.6	0.402	7.213	0.496	4.286	4.616	0.928
SQVR-4	13.0	0.386	5.383	0.356	3.454	3.753	0.920
SQVR-6	13.9	0.356	3.295	0.201	2.642	2.957	0.893
SQVR-8	17.5	0.258	1.413	0.062	1.845	2.375	0.776
SQVR residue	30.0	0.066	0.723	0.0082	0.762	1.584	0.481
SQVR	14.7	0.335	3.134	0.179	1.840	2.009	0.915
SQVR	14.7	0.334	3.134	0.179	2.077	2.293	0.905

Table 1B HDN diffusivities and kinetic parameters of SFEF fractions

feed	$d_r/\text{\AA}$	$F(\lambda)$	$D_b/10^{-10}\text{m}^2\text{s}^{-1}$	$D_e/10^{-10}\text{m}^2\text{s}^{-1}$	$k/10^{-4}\text{ms}^{-1}$	$k_p/10^{-4}\text{ms}^{-1}$	$\eta$
DGAR-1	9.34	0.522	112.2	10.01	8.520	8.582	0.992
DGAR-2	9.71	0.507	93.53	8.109	8.350	8.423	0.991
DGAR-3	10.1	0.492	85.27	7.175	5.857	5.898	0.993
DGAR-4	10.3	0.483	76.00	6.274	5.285	5.324	0.992
DGAR-5	10.6	0.474	72.30	5.858	4.392	4.420	0.993
DGAR-6	10.8	0.462	63.83	5.046	4.016	4.043	0.993
DGAR-7	11.3	0.445	51.71	3.936	2.634	2.650	0.994
DGAR-8	12.2	0.413	27.55	1.946	1.851	1.866	0.991
DGAR residue	20.2	0.198	2.116	0.072	0.502	0.533	0.941
DGAR	11.0	0.456	62.23	4.856	1.523	1.527	0.997
SZVR-1	11.2	0.448	38.48	2.949	2.357	2.376	0.992
SZVR-2	12.5	0.402	7.207	0.495	2.160	2.217	0.974
SZVR-3	13.1	0.385	6.894	0.454	1.338	1.383	0.971
SZVR-4	13.6	0.367	5.141	0.322	1.341	1.402	0.956
SZVR-5	14.5	0.339	3.415	0.197	0.833	0.650	0.973
SZVR-6	14.8	0.332	2.582	0.146	0.615	0.638	0.964
SZVR-7	17.1	0.269	1.761	0.081	0.400	0.417	0.958
SZVR residue	31.7	0.053	0.772	0.0069	0.215	0.281	0.766
SQVR-2	12.6	0.402	7.213	0.496	1.049	1.068	0.982
SQVR-4	13.0	0.386	5.383	0.356	0.799	0.815	0.980
SQVR-6	13.9	0.356	3.295	0.201	0.465	0.475	0.980
SQVR-8	17.5	0.258	1.413	0.062	0.158	0.162	0.978

The molecular size of SEFE fractions is 10-20Å and 20-30Å for the SEFE residue. The largest ratio of diffusion molecule diameter to pore diameter is 0.48, which is less than 0.5. In the present study conditions, bulk diffusivity is  $0.7 \sim 112 \times 10^{-10} \text{ m}^2/\text{s}$ , and the effective diffusivity is  $0.006 \sim 10 \times 10^{-10} \text{ m}^2/\text{s}$ . The bulk diffusivity varies within the range of liquid diffusivity for less viscous system. The effective diffusivity belongs to the range of configuration [16]. For less viscous system the diffusivity agrees with that in reference very well [17], but for more viscous system, no published data can be used to compare.

The apparent and intrinsic rate constants are  $0.76 \sim 9.25 \times 10^{-12} \text{ m/s}$  and  $1.58 \sim 9.32 \times 10^{-12} \text{ m/s}$  for HDS, and  $0.15 \sim 8.52 \times 10^{-12} \text{ m/s}$  and  $0.16 \sim 8.58 \times 10^{-12} \text{ m/s}$  for HDN. For the same feed, HDS reaction rate is always greater than HDN. Which means that the removal of nitrogen is more difficult than that of sulfur in heavy oil.

The differences of rate constants between HDS and HDN for different feeds are shown in figure 2. Such differences are obviously greater for medium fractions than for lighter and heavier fractions. It may be ascribed to the difficulty for lighter fraction reaching to high conversion of HDS reaction and for the removal of sulfur and nitrogen of heavier fraction with high aromaticity. Therefore, the deeply HDS of lighter fraction is very difficult as the HDS and HDN of heavier fraction.

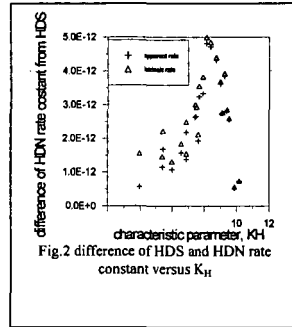


Fig.2 difference of HDS and HDN rate constant versus  $K_H$

Figure 3 and 4 shows the relationships of apparent and intrinsic rate constant of HDS and HDN and the heavy oil characteristic parameter<sup>[18]</sup>,  $K_H$ , and the molecular weight of feed. The apparent and intrinsic rate constants decrease quickly with the increase of AMW, and reach to a stable value. Rate constants vary with the decrease of  $K_H$  with the similar mode mentioned above, and the minimum value in close to the level of thermal cracking. It is better to describe the HDS and HDN reactivity of SEFE fractions with the heavy oil characteristic parameter than AMW. The intrinsic reactivity decreases most quickly at  $K_H=8.0$  for HDS reaction, and quickly at the startup of  $K_H=9.5$ . This phenomenon agrees with the common views that the HDS reactivity is obvious greater than that of HDN for lighter distillate.

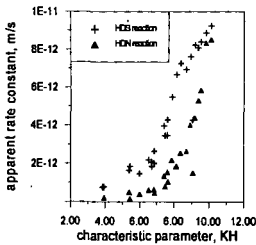


Fig.3A  $k_a$  versus  $K_H$

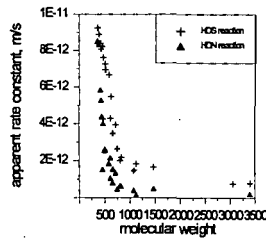


Fig.3B  $k_a$  versus AMW

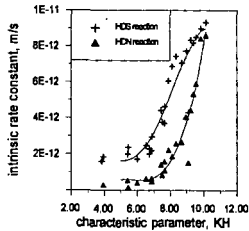


Fig.4A  $k_i$  versus  $K_H$

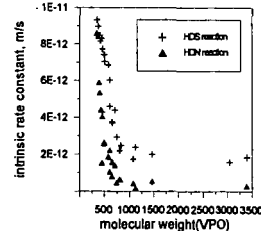


Fig.4B  $k_i$  versus AMW

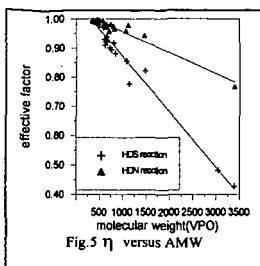


Figure 5 is the plots of relationships of effectiveness factors of HDS and HDN and the molecular weight of feed. The effectiveness factors decrease proportionally with the increase of AMW. This means that diffusion effect exists in the present reaction conditions, and the heavier the fraction is, the larger the molecular size, and the severer the diffusion effect.

With the increase of fraction AMW, the decrease of intrinsic rate constant for HDN is faster than for HDS, but the decrease of effectiveness factor for HDN is slower than for HDS. Therefore, the poorer HDS and HDN reactivity for heavier fractions can be explained by the lower intrinsic reactivity as

well as stronger diffusion resistance, and the decrease of intrinsic reactivity is the controlling factor for HDN reaction.

## CONCLUSION

Through the catalytical hydroconversion of SFEF fractions which properties change in a large range, some conclusions were emerged. The diffusion of macromolecule in catalyst micropore filled with liquid belongs to configuration diffusion. The HDS and HDN diffusion-reaction model of residue in autoclave reactor was established. The intrinsic and apparent rate constants of HDS and HDN reaction obtained in terms of the kinetic model decrease quickly and reach to stable values with the increase of average molecular weight. HDN rate constant declines faster than that of HDS, but the effective factor of HDS decreases more quickly than that of HDN. It means that the low conversion of HDS and HDN reaction for heavier SFEF fractions could be ascribed to the poorer reactivity and the stronger diffusion resistance. The heavier the SFEF fraction, the larger the molecular size, and the severer the effect of diffusion on the reaction.

## REFERENCES

1. Hoog H. *J Inst Petro.* 1950,36:738
2. Yitzhaki D, Aharoni C. *AIChE J.* 1988,23:342
3. Philippopoulos C, Papayannkos N. *IEC Res.* 1988,27(3):415
4. Trytten L C, Gray M R. *IEC Res.* 1990,29(5):725
5. Dai wenguo. The catalytic cracking characteristics of resins in different narrow fractions of Shengli vacuum residuum. Master thesis, University of Petroleum, China. March 1993
6. Chang Jie, Kinetics and Catalyst Deactivity Model of Residua. Doctoral thesis, Beijing Research Institute of Petroleum Processing, China, August 1997
7. Shah Y T, Paraskas J A. *ICE Press Des.Dev.* 1975, 14(4):368
8. Levenspiel O. *Chemical Reaction Engineering(second edition)*. John Wiley & Sons, Inc. 1972, P474
9. Ruckenstein E, Tsai M C. *AIChE J.* 1981, 27(4):697
10. Chen Gantong, *Chemical Reaction Engineering(Chinese)*. Chemical Industry Press, July 1981, P182
11. Carberry J J, *Chemical Reaction and Reactor Engineering*. Marcel Dekker, Inc. 1987, P251
12. Renkin E M. *Journal of General Physiology.* 1954, 38:225
13. Yang Chaohe. Characteristics and kinetics of heavy oil Hydroconversion. Doctoral Thesis, University of petroleum, Beijing, China, 1997
14. Shi Jun. *Handbook of Chemical Engineering(section 10)Mass Transfer*. Chemical Industry Press, October 1989, P10-80
15. Chen Y W, Thasi M C. *IEC Res.* 1995, 34:898
16. Weisy P B. *Chem. Techn.* 1973:504
17. Baltus R E. *Fuel Sci & Techn.Intl.* 1993, 11(5&6):52
18. Si Tiepan, Hu Yunxiang, et al. *Acta Petrolei Sinica(Petroleum Processing Section)*. 1997, 13(2):1